Renal expression of parvalbumin is critical for NaCl handling and response to diuretics

Hendrica Belge*, Philippe Gailly†, Beat Schwaller‡, Johannes Loffing‡, Huguette Debaix*, Eva Riveira-Munoz*, Renaud Beauwens§, Jean-Pierre Devogelaer¶, Joost G. Hoenderop‖, René J. Bindels‖, and Olivier Devuyst*,**

Departments of *Nephrology, †Physiology, and ¶Rheumatology, Université Catholique de Louvain Medical School, B-1200 Brussels, Belgium; ‡Unit of Anatomy, University of Fribourg, CH-1700 Fribourg, Switzerland; §Laboratory of Cell and Molecular Physiology, Université Libre de Bruxelles Medical School, B-1070 Brussels, Belgium; and ‖Department of Physiology, Radboud University Nijmegen, 6500 HC Nijmegen, The Netherlands

The distal convoluted tubule (DCT) plays an essential role in the reabsorption of NaCl by the kidney, a process that can be inhibited by thiazide diuretics. Parvalbumin (PV), a Ca^{2+}-binding protein that plays a role in muscle fibers and neurons, is selectively expressed in the DCT, where its role remains unknown. We therefore investigated the renal phenotype of PV knockout mice ($Pvalb^{-/-}$) vs. wild-type ($Pvalb^{+/+}$) littermates. PV colocalized with the thiazide-sensitive Na^+-Cl^- cotransporter (NCC) in the early DCT. The $Pvalb^{-/-}$ mice showed increased diuresis and kaliuresis at baseline with higher aldosterone levels and lower lithium clearance. Acute furosemide administration increased diuresis and natriuresis/kaliuresis, but, surprisingly, did not increase calciuria in $Pvalb^{-/-}$ mice. NaCl supplementation of $Pvalb^{-/-}$ mice increased calciuria at baseline and after furosemide. The $Pvalb^{-/-}$ mice showed no significant diuretic response to hydrochlorothiazide, but an accentuated hypocalciuria. A decreased expression of NCC was detected in the early DCT of $Pvalb^{-/-}$ kidneys in the absence of ultrastructural and apoptotic changes. The PV-deficient mice had a positive Ca^{2+} balance and increased bone mineral density. Studies in mouse DCT cells showed that endogenous NCC expression is Ca^{2+}-dependent and can be modulated by the levels of PV expression. These results suggest that PV regulates the expression of NCC by modulating intracellular Ca^{2+} signaling in response to ATP in DCT cells. They also provide insights into the Ca^{2+}-sparing action of thiazides and the pathophysiology of distal tubulopathies.

distal convoluted tubule | kidney | salt-losing nephropathy | sodium-chloride cotransport

Parvalbumin (PV) belongs to the superfamily of EF-hand Ca^{2+}-binding proteins that play a role in multiple cellular processes, including gene transcription, ion transport, protein phosphorylation, and enzymatic activities (1). These proteins possess well conserved helix–loop–helix motifs that bind Ca^{2+} ions with high affinity, leading to conformational changes. The conformational plasticity and the cell-specific expression of these Ca^{2+} sensor or buffer proteins contribute to the versatility of Ca^{2+} signaling (2). PV is a 109-aa cytosolic protein that contains a pair of functional EF-hand motifs forming a stable unit that binds two Ca^{2+} ions (3). This Ca^{2+} buffer is expressed in a restricted number of vertebrate tissues, including fast-contracting/relaxing skeletal muscle fibers and GABA neurons in the brain (4). The generation of PV knockout ($Pvalb^{-/-}$) mice confirmed the important role played by PV in muscle and brain (5). The fast muscles of $Pvalb^{-/-}$ mice exhibit a decreased relaxation rate of the twitch (5), suggesting that PV facilitates Ca^{2+} diffusion from myofibrils to the sarcoplasmic reticulum (6). The lack of PV in the brain induces changes in short-term synaptic plasticity and modified network properties, resulting in increased susceptibility to epileptic seizures (7). Although no human disease is associated with the *PVALB* gene on 22q12-q13.1, reduced GABA synthesis in PV-containing neurons has been evidenced in individuals with schizophrenia and impaired cognitive functions (8).

In addition to muscle fibers and neurons, PV is expressed in epithelial cells lining the distal convoluted tubule (DCT) in rat and mouse kidney (9, 10). The DCT reabsorbs ≈5% of the filtered load of Na^+, a process that involves the Na^+-Cl^- cotransporter (NCC) and the ClC-Kb chloride channel, located on the apical and basolateral membrane of the cells, respectively. The reabsorption of NaCl is inhibited by thiazide diuretics, which probably compete for the Cl^- binding site of the apical NCC (11). The DCT also plays a key role in the active Ca^{2+} reabsorption in the distal nephron, through a transcellular pathway that involves passive entry of Ca^{2+} via the apical channel TRPV5, cytosolic diffusion to Ca^{2+}-binding calbindins (CBs; CB-D28k and CB-D9k) and active basolateral extrusion through Na^+-Ca^{2+} exchanger 1 and plasma membrane Ca^{2+}-ATPase 1b (PMCA1b) (12). Furthermore, the DCT is involved in the final reabsorption of Mg^{2+} through the apical channel TRPM6 and a basolateral active transport (12). The selective distribution of PV in the early part of the DCT, and its unique Ca^{2+} buffering properties, raised the question of whether it may play a role in the transport systems operating in that nephron segment.

In this study, we used $Pvalb^{-/-}$ mice to investigate the effects of PV on renal handling of NaCl and divalent cations in basal conditions and after acute administration of diuretics and NaCl repletion. The PV-deficient mice are characterized by a decreased expression of NCC in the early DCT, leading to a discrete NaCl-losing phenotype with impaired response to diuretics, and positive Ca^{2+} balance with increased bone mineral content and resistance. The functional relationship between PV and NCC was further studied in mouse DCT (mDCT) cells, revealing that PV modulates the Ca^{2+} transients induced by ATP and regulates the endogenous expression of NCC.

Results

PV Is Distributed in the Early DCT of Mouse and Human. The cytoplasmic staining for PV was detected in a subset of tubules located in the outer cortex of $Pvalb^{+/+}$ kidneys (Fig. 1A). All PV-positive segments showed apical NCC staining, thus confirming the distribution of NCC in the DCT. However, PV is restricted to the early part of the DCT, whereas NCC is expressed along the entire DCT, and CB-D28k is more abundant in the distal part of the DCT and
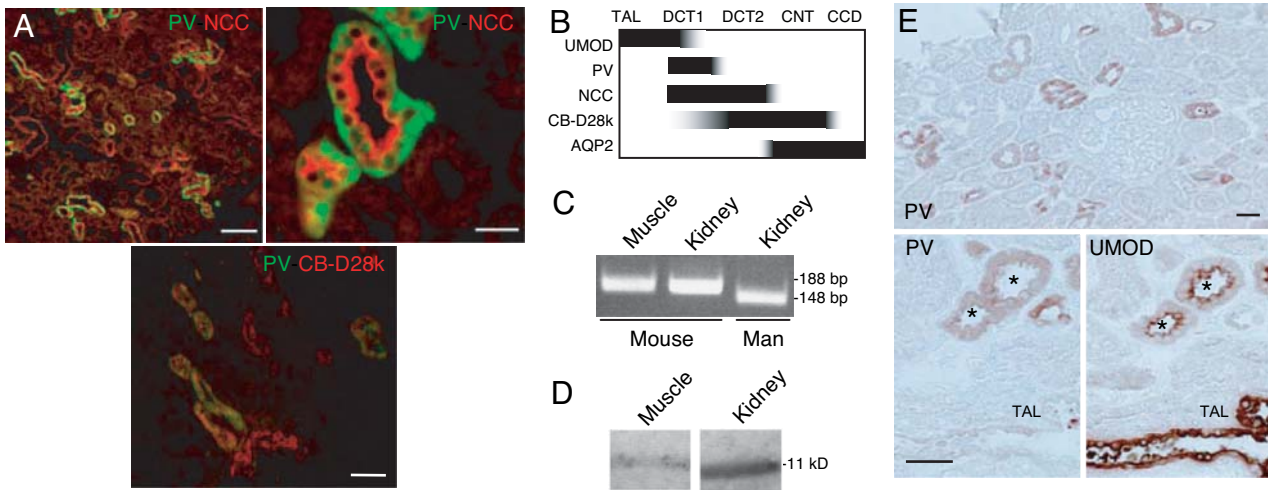

Fig. 1. Expression and distribution of PV in mouse and human kidney. (*A*) Double immunofluorescence staining of mouse kidney cortex sections showing immunopositive staining for PV and NCC and PV and CB-D28k. Note the different expression pattern of PV (cytosolic) and NCC (apical). (*B*) Distribution of uromodulin (UMOD), PV, NCC, CB-D28k, and AQP2 along the nephron. TAL, thick ascending limb of Henle's loop; DCT1, early part of the DCT; DCT2, late part of DCT; CNT, connecting tubule; CCD, cortical collecting duct. (*C*) RT-PCR detection of PV in muscle and kidney samples from mouse and human (20 μl of PCR product per lane). (*D*) Immunoblotting of PV (11 kDa) in cytosolic extracts from mouse muscle and human kidney. (*E*) In human kidney, PV colocalizes with UMOD in the early DCT (∗) following the TAL. (Scale bars: 100 μm, *A Upper Left*; 20 μm, *A Upper Right*; and 50 μm, *A Lower* and *E*.)

the connecting tubule (Fig. 1*B*). The deletion of PV was not reflected by structural and histological abnormalities in the kidney [supporting information (SI) Fig. 6]. PV was also detected in the human kidney (Fig. 1 *C* and *D*), located within the early DCT identified by codistribution with uromodulin (Fig. 1*E*).

***Pvalb*$^{-/-}$ Mice Show Polyuria, Polydipsia, and Increased Kaliuresis.** At baseline, *Pvalb*$^{-/-}$ mice exhibited increased kaliuresis, decreased lithium clearance, increased aldosteronuria, and a trend for reduced calciuria, whereas magnesiuria and phosphaturia were unchanged (Table 1). Body weight, hematocrit, renal function, acid/base status, plasma osmolality, and electrolyte values were similar in both genotypes. The *Pvalb*$^{-/-}$ mice had a significant polyuria, with diluted urine and higher fluid intake (*Pvalb*$^{-/-}$: 8.0 ± 1 vs. *Pvalb*$^{+/+}$:

4.1 ± 0.3 ml/24 h, $n = 6$ pairs, $P = 0.002$). Water deprivation induced a similar antidiuresis (SI Fig. 7), ruling out a defective urinary concentrating mechanism. The *Pvalb*$^{-/-}$ mice had higher plasma 1,25(OH)$_2$D$_3$ levels, with a trend for lower ionized Ca^{2+} levels (Table 1).

Impaired Response to Furosemide and NaCl Supplementation in *Pvalb*$^{-/-}$ Mice. Furosemide was injected in *Pvalb* mice to increase NaCl and Ca^{2+} delivery to the DCT and test the role of PV in that segment (Fig. 2). The anticipated diuretic response was observed in both groups (Fig. 2*A*), paralleled by increased natriuria and kaliuria (Fig. 2 *B* and *C*). Surprisingly, the furosemide-induced hypercalciuria, as observed in *Pvalb*$^{+/+}$ mice, was absent in *Pvalb*$^{-/-}$ mice (Fig. 2*D*). The *Pvalb*$^{-/-}$ mice were then NaCl-repleted (Fig. 2 *E* and *F*)

Table 1. Biological parameters at baseline in *Pvalb* mice

Measurement	*Pvalb*$^{+/+}$	*Pvalb*$^{-/-}$	P
Blood/plasma			
Osmolality, mOsm/kg H$_2$O	323 ± 5	324 ± 3	0.98
Hematocrit, %	46 ± 1.7	43 ± 1.4	0.27
Creatinine, mg/dl	0.25 ± 0.02	0.28 ± 0.02	0.26
Urea, mg/dl	24 ± 2	27 ± 2	0.22
Na$^+$, mM	141 ± 1	142 ± 0.4	0.42
K$^+$, mM	6.1 ± 0.2	5.3 ± 0.4	0.18
Mg^{2+}, mM	2.5 ± 0.2	2.8 ± 0.2	0.32
tCO$_2$, mM	24 ± 1	22 ± 0.4	0.16
Ionized Ca^{2+}, mM	1.28 ± 0.02	1.23 ± 0.02	0.11
1,25(OH)$_2$D$_3$, pg/ml	112 ± 9	177 ± 13*	0.001
Urine			
Diuresis, μl/min·g body weight	0.03 ± 0.01	0.05 ± 0.01*	0.03
Osmolality, mOsm/kg H$_2$O	3861 ± 384	2610 ± 226*	0.02
Na$^+$/creatinine, nmol/ng creatinine	0.36 ± 0.03	0.35 ± 0.03	0.85
K$^+$/creatinine, nmol/ng creatinine	0.35 ± 0.01	0.43 ± 0.03*	0.045
Ca^{2+}/creatinine, ng/ng creatinine	0.70 ± 0.10	0.51 ± 0.12	0.25
Mg^{2+}/creatinine, ng/ng creatinine	0.74 ± 0.05	0.76 ± 0.06	0.80
Fractional excretion, PO$_4$$^{2-}$	67 ± 14	72 ± 11	0.78
Lithium clearance, μl/min	19.1 ± 1.60	12.5 ± 1.32*	0.01
Aldosterone, μmol/min	6.5 ± 1.6	18 ± 9.9*	0.02

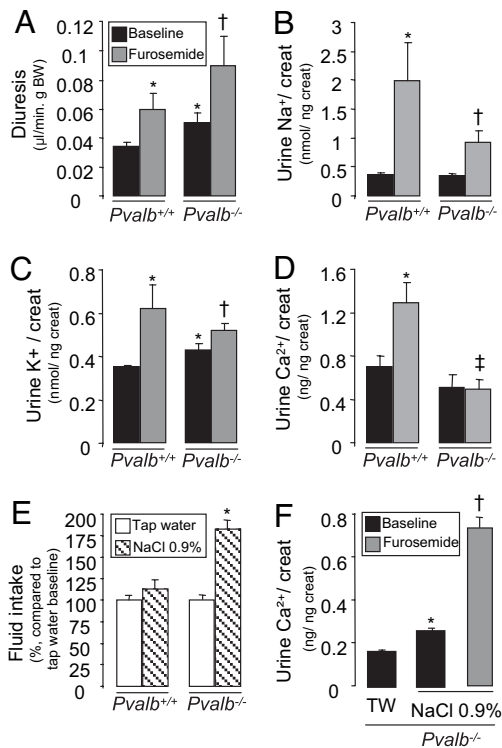∗, $P < 0.05$ versus *Pvalb*$^{+/+}$; $n = 6$ pairs.

2

Fig. 2. Furosemide testing and NaCl supplementation in *Pvalb* mice. (*A–D*) Furosemide injection induces an increase in diuresis (*A*), natriuresis (*B*), and kaliuresis (*C*), but no hypercalciuria (*D*) in the *Pvalb*$^{-/-}$ mice. *, $P < 0.05$ vs. *Pvalb*$^{+/+}$ baseline; †, $P < 0.05$ vs. *Pvalb*$^{-/-}$ baseline; ‡, $P < 0.05$ vs. *Pvalb*$^{+/+}$ furosemide. (*E*) *Pvalb*$^{-/-}$ mice show a higher avidity for NaCl solution during a 48-h supplementation, compared with *Pvalb*$^{-/-}$ mice receiving tap water. No such avidity is observed in *Pvalb*$^{+/+}$ mice. (*F*) Exposure of *Pvalb*$^{-/-}$ mice to oral NaCl supplementation increases calciuria at baseline and leads to the expected furosemide-induced hypercalciuria. *, $P < 0.05$ vs. tap water (TW); †, $P < 0.05$ vs. baseline ($n = 6$ in each group).

to investigate whether the lower calciuria at baseline and the lack of furosemide-induced hypercalciuria could reflect volume depletion and compensatory NaCl and Ca^{2+} reabsorption in the proximal tubule (PT), as suggested by the lower lithium clearance. The *Pvalb*$^{-/-}$ mice showed a striking avidity for the NaCl solution (+82% fluid intake, as compared with the usual tap water) that was not observed in *Pvalb*$^{+/+}$ mice (Fig. 2*E*). Short- and long-term NaCl supplementation induced a significant increase in diuresis, natriuresis, calciuria, and magnesiuria in *Pvalb*$^{-/-}$ mice (SI Table 2). Administration of furosemide to the NaCl-repleted *Pvalb*$^{-/-}$ mice led to the anticipated increase of calciuria (+195%; Fig. 2*F*), which, however, remained lower than the values observed in *Pvalb*$^{+/+}$ mice.

Impaired Response to Thiazide and Accentuated Hypocalciuria in *Pvalb*$^{-/-}$ Mice. A single dose of hydrochlorothiazide (HCTZ) was injected to directly test the DCT (Fig. 3). The *Pvalb*$^{+/+}$ mice showed the expected diuretic response, with natriuresis and a trend for decreased calciuria (Fig. 3 *A–D*). Strikingly, the *Pvalb*$^{-/-}$ mice showed no diuretic response (Fig. 3*A*), contrasting with a significant hypocalciuria (Fig. 3*D*). The time-dependent effect of HCTZ on the urinary excretion of Na^+ and Ca^{2+} was investigated (Fig. 3 *E* and *F* and SI Table 3). In *Pvalb*$^{+/+}$ mice, Na^+ excretion significantly increased during the first 6 h after HCTZ, whereas calciuria was unchanged. During the next 6 h, a significant decrease of natriuria and calciuria was observed. In contrast, *Pvalb*$^{-/-}$ mice already showed a marked hypocalciuria during the first 6 h without signif-
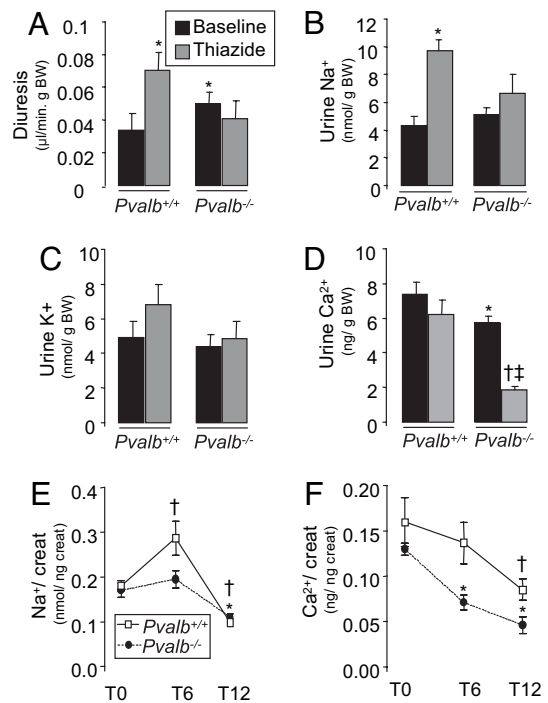

Fig. 3. Response to thiazide in *Pvalb* mice. (*A–D*) Diuresis (*A*), natriuresis (*B*), kaliuresis (*C*), and calciuria (*D*) in six pairs of *Pvalb* mice at baseline and after HCTZ is shown. The *Pvalb*$^{-/-}$ mice show no significant diuretic response but an accentuated hypocalciuria after HCTZ. *, $P < 0.05$ vs. *Pvalb*$^{+/+}$ baseline; †, $P < 0.05$ vs. *Pvalb*$^{-/-}$ baseline; ‡, $P < 0.05$ vs. *Pvalb*$^{+/+}$ furosemide. (*E* and *F*) Time course of Na^+ (*E*) and Ca^{2+} (*F*) excretion 6 and 12 h after a single HCTZ injection ($n = 9$ pairs). In *Pvalb*$^{+/+}$ mice, Na^+ excretion significantly increases during the first 6 h, with unchanged calciuria. During the next 6 h, a significant hypocalciuria occurs, paralleled by a decreased natriuria. In *Pvalb*$^{-/-}$ mice, a significant hypocalciuria is detected during the first 6 h, without change in natriuria. The hypocalciuria is accentuated during the next 6 h, paralleled by a decrease in natriuria. †, $P < 0.05$ vs. *Pvalb*$^{+/+}$ baseline; *, $P < 0.05$ vs. *Pvalb*$^{-/-}$ baseline.

icant natriuresis. The hypocalciuria was accentuated during the next 6 h, paralleled by a significant decrease of natriuria.

Taken together, the significant alterations observed in the *Pvalb*$^{-/-}$ mice at baseline and in response to loop and thiazide diuretics hinted at a molecular defect in the DCT inducing several tubular compensatory mechanisms.

The Deletion of PV Decreases the Expression of NCC in the DCT. To investigate the potential mechanisms responsible for the phenotype of *Pvalb*$^{-/-}$ mice, we analyzed the renal expression of genes involved in distal tubular transport (Fig. 4*A*). A 3-fold decrease in the mRNA encoding NCC, paralleled by a 2-fold decrease in WNK4 and the kidney-specific WNK1, was observed in *Pvalb*$^{-/-}$ kidneys. In contrast, the mRNA levels of renin and neuronal nitric-oxide synthase (nNOS) were up-regulated in *Pvalb*$^{-/-}$ kidneys, whereas Na^+-K^+-ATPase, TRPV5, CB-D28k, PMCA1b, Na^+-Ca^{2+} exchanger 1, and ClC-Kb levels were unchanged. Immunoblotting confirmed the decreased expression of NCC in *Pvalb*$^{-/-}$ kidneys (Fig. 4*B*), with a weaker staining intensity and a lower apical recruitment when compared with *Pvalb*$^{+/+}$ mice (Fig. 4*C*). The few remaining profiles showing apical NCC staining were strongly positive for CB-D28k, indicating that they belong to the distal part of the DCT that does not express PV *in vivo* (data not shown). Treatment with high-dose thiazide has been associated with atrophy of the DCT epithelium and massive apoptotic cell death (13). However, EM analysis did not show significant remodeling of the DCT cells in *Pvalb*$^{-/-}$ mice, and negative TUNEL and
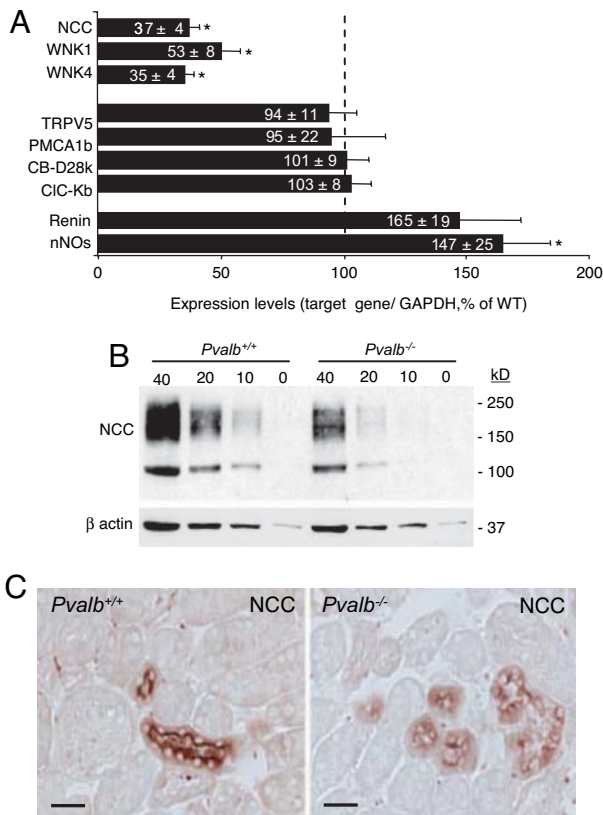
Fig. 4. Decreased expression of NCC in $Pvalb^{-/-}$ mice. (*A*) Quantification (real-time PCR) of target mRNAs in $Pvalb^{-/-}$ kidneys, expressed as relative expression over $Pvalb^{+/+}$ kidneys ($n = 4$ pairs). There is a significant down-regulation of NCC, WNK4, and kidney-specific WNK1 and an up-regulation of nNOS and renin ($P = 0.14$) in $Pvalb^{-/-}$ kidneys. *, $P < 0.05$ vs. $Pvalb^{+/+}$. (*B*) Immunoblotting of NCC in extracts from *Pvalb* kidneys. Serial dilutions of total kidney homogenates were subjected to SDS/PAGE analysis and incubated with anti-NCC antibodies. A ≈2-fold decreased expression of NCC is detected in the $Pvalb^{-/-}$ kidneys. (*C*) Immunostaining for NCC. In comparison with the strong apical staining observed in $Pvalb^{+/+}$ mice, a weaker and mostly intracellular staining for NCC is detected in DCT of $Pvalb^{-/-}$ mice. (Scale bars: 50 μm.)

poly(ADP-ribose)polymerase cleavage assays ruled out increased apoptosis (SI Fig. 8).

Pvalb$^{-/-}$ Mice Show Bone Modifications. Increased bone mineral density is observed in association with thiazide treatment (14) and in NCC-deficient mice and Gitelman's syndrome (GS) patients (15). We thus investigated whether the hypocalciuria and reduced expression of NCC in Pvalb$^{-/-}$ mice were likewise associated with a bone phenotype. Detailed computed tomography analyses showed a significant increase in the trabecular mineral content and the periostal circumference and a higher mechanical resistance (axial moment of inertia) in the proximal tibia of $Pvalb^{-/-}$ mice (SI Fig. 9 and SI Table 4).

PV and Ca^{2+} Signaling Regulate the Expression of NCC in mDCT Cells.
The mechanism by which PV could regulate NCC expression was investigated in mDCT cells (16, 17), which endogenously express PV and NCC (Fig. 5). We transfected the cells with various siRNA against PV and showed that the knockdown of PV induces a significant decrease in the expression of NCC (Fig. 5*A*). Inversely, a strong and specific induction of NCC expression was observed in different clones stably transfected with PV (Fig. 5*B*). Because DCT cells are sensitive to P2 receptor-mediated purinergic signaling (18), we tested whether PV could modulate ATP-induced Ca^{2+} tran-
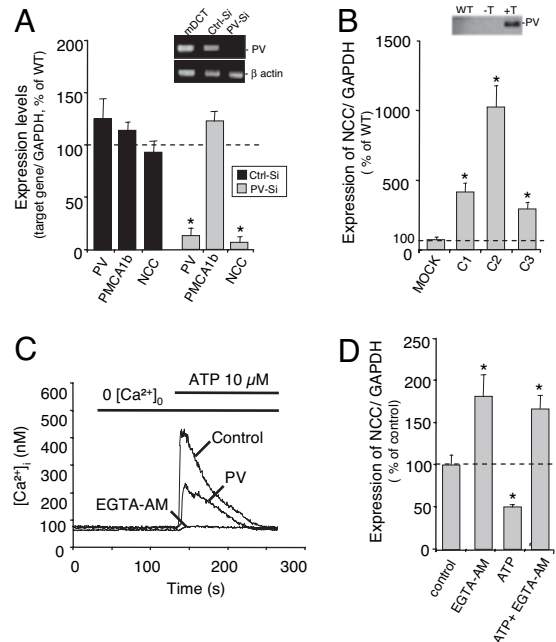

Fig. 5. Role of PV and Ca^{2+} signaling in mDCT cells. (*A*) Characterization of siRNA-treated mDCT cells. Cells treated with PV-siRNA show a significant decrease in the expression of PV and NCC, whereas PMCA1b is unchanged. Untreated cells and cells treated with control siRNA clearly express PV as shown by PCR (*Inset*) and do not show any significant change in PMCA1b and NCC expression. Similar results were obtained with three different siRNAs. *, $P < 0.05$ vs. control siRNA. (*B*) Expression of NCC in cells stably transfected with PV. The expression level of NCC is significantly increased in three different clones (C1–C3) overexpressing PV, in comparison to mock-transfected cells. *, $P < 0.05$ vs. mock. (*Inset*) Immunoblot analysis (anti-GFP antibody) showing the PV-GFP protein in stably transfected cells but not in WT and control-transfected cells. (*C*) Stimulation of mDCT cells with 10 μM ATP induced a release of Ca^{2+} (no [Ca^{2+}]$_0$, 0.5 mM EGTA). ATP-induced [Ca^{2+}]$_i$ transients were reduced in cells overexpressing PV or mDCT cells preincubated for 6 h in the presence of 10 μM EGTA-AM. (*D*) Expression of NCC is Ca^{2+}-dependent. Cells incubated for 6 h with 10 μM EGTA-AM showed an increased expression of NCC. Repetitive stimulation with 10 μM ATP induced a 2-fold decrease of NCC expression; the effect was lost when cells were preincubated with EGTA-AM. *, $P < 0.05$ vs. control.

sients and NCC expression. Having confirmed the expression of P2X and P2Y2 receptors by RT-PCR (data not shown), we showed that 10 μM ATP induces Ca^{2+} transients in mDCT cells (Fig. 5*C*). The transients were significantly reduced in cells stably transfected with PV and cells exposed to the permeable Ca^{2+} chelator EGTA-AM. In parallel, we observed a 2-fold induction of NCC expression in cells incubated with EGTA-AM, whereas stimulation with ATP decreased the expression of NCC (Fig. 5*D*). The latter effect was not observed in cells preincubated with EGTA-AM, demonstrating the negative control that Ca^{2+} transients exert on NCC expression. The expression of PV and PMCA1b was unchanged in these conditions.

Discussion

Our studies reveal that PV is critical for renal NaCl and Ca^{2+} handling and the response to diuretics in mouse, by modulating the Ca^{2+} transients induced by ATP and regulating the endogenous expression of NCC in DCT cells. These results are relevant when considering the role of the DCT, the action of diuretics, and the pathophysiology of distal tubulopathies.

Because the distribution of PV in kidney has been debated (10, 19), we confirmed that PV is restricted to the early DCT, where it colocalizes with NCC. The deletion of PV entailed a discrete, but consistent, phenotype. At baseline, $Pvalb^{-/-}$ mice showed a poly-

uria probably caused by polydipsia, because the urinary concentrating ability was unchanged. Their endogenous lithium clearance was decreased, reflecting enhanced Na^+ reabsorption in PT (20), with higher aldosterone levels, increased kaliuria, and increased expression of nNOS and renin, suggestive of volume depletion. The $Pvalb^{-/-}$ mice had similar body weight, hematocrit, and plasma electrolyte levels compared with $Pvalb^{+/+}$ mice, indicating that compensatory mechanisms were efficient. Unexpectedly, treatment of $Pvalb^{-/-}$ mice with furosemide did not result in hypercalciuria, indicating a dissociation of the natriuretic and calciuretic response. Because hypovolemia triggers a compensatory PT reabsorption of Na^+ and Ca^{2+}, we conjectured that extracellular volume depletion could play a role in the altered Ca^{2+} handling in response to furosemide. Indeed, NaCl-supplemented $Pvalb^{-/-}$ mice increased their baseline calciuria (which, however, remained lower than in $Pvalb^{+/+}$ mice; see Fig. 2) and showed the expected furosemide-induced hypercalciuria. These data indicate a close relationship between the extracellular volume status and the effect of loop diuretics and a cross-talk between distal and proximal nephron segments reflected in the tubular handling of Na^+ and Ca^{2+}.

Analysis of $Pvalb^{-/-}$ mice yielded information about the response to thiazides. Administration of HCTZ to $Pvalb^{-/-}$ mice resulted in two remarkable features: a lack of diuretic response and a significantly accentuated hypocalciuric effect. The impaired diuretic response probably reflects the decreased NCC expression in the DCT (see Fig. 4) and compensatory reabsorption of Na^+ in both PT and collecting ducts (aldosterone-induced). The fact that HCTZ induced a profound hypocalciuria without affecting natriuresis is particularly relevant. Studies in NCC-null mice (20) and rats treated with high-dose HCTZ (21) demonstrated that enhanced PT-passive Ca^{2+} transport contributes to thiazide-induced hypocalciuria. The negative lithium clearance (and higher nNOS, renin, and aldosterone levels suggestive of volume contraction) indicates that the latter mechanism probably operates in $Pvalb^{-/-}$ mice. However, our data suggest that an effect within the DCT is also important. First, time-course analyses showed that, in $Pvalb^{-/-}$ mice, HCTZ induces an early hypocalciuria without affecting natriuresis. Second, when $Pvalb^{-/-}$ mice are salt-repleted, their urinary calcium/creatine ratio remains lower (≈ 0.75) than in wild-type mice (≈ 1.3). These results indicate that thiazide-induced hypocalciuria may occur without extracellular volume contraction, consistent with a mouse model of chronic treatment with lower doses of thiazide (22). Several models with enhanced PT-passive Ca^{2+} reabsorption are characterized by profound structural damage of the DCT and/or a reduced expression of molecules involved in the distal Ca^{2+} transport (20, 21, 23). In contrast, the $Pvalb^{-/-}$ mice have an intact DCT, which could be caused by the residual expression of NCC, and the expression of molecules involved in distal Ca^{2+} transport is unchanged or even increased (CB-D9k) (B.S., unpublished data). At any rate, PV is not required for Ca^{2+} reabsorption: the coexistence of hypocalciuria with unchanged plasma Ca^{2+} levels indicated Ca^{2+} accumulation in $Pvalb^{-/-}$ mice and bone mineral density was increased, as reported in NCC-deficient mice and GS patients (15).

Although the salt-losing phenotype of the $Pvalb^{-/-}$ mice bears some resemblance with the NCC-deficient mice (23, 24), there are differences between the strains. The $Pvalb^{-/-}$ mice had polyuria and polydipsia at baseline, possibly related to increased kaliuria and a trend toward hypokalemia. A central component may also interfere, because PV is distributed in the brain and $Pvalb^{-/-}$ mice manifest a subtle locomotor phenotype (25). The NCC-null mice had no disturbance of K^+ homeostasis at baseline, but developed inappropriate kaliuria, hypokalemia, polyuria, and polydypsia when exposed to a low K^+ diet (26). The $Pvalb^{-/-}$ mice have no hypomagnesemia without specific provocation, consistent with the lack of structural changes in the DCT. In contrast, NCC knockout mice show renal Mg^{2+} wasting and hypomagnesemia at baseline, likely caused by the severe damage in the DCT causing a loss in TRPM6-expressing cells (23, 24). Genetic backgrounds, which are important for the NCC-null phenotype (23, 24, 26), may also play a role in differences between strains.

The lack of PV in the kidney was associated with a marked down-regulation of NCC, with reduced apical targeting in most of the DCT, in the absence of structural changes or apoptosis. The few remaining tubule profiles showing apical NCC were strongly positive for CB-D28k, indicating their appartenance to the distal part of the DCT that does not express PV *in vivo*. A reduced mRNA level was also observed for WNK4 and the kidney-specific WNK1, two serine/threonin kinases that interact to control NCC activity in the DCT (27, 28). The decreased expression of both WNK4 and WNK1 may thus constitute a compensatory mechanism (29) to counteract the reduced expression of NCC in $Pvalb^{-/-}$ mice.

The potential link between PV and NCC was investigated in mDCT cells. The knockdown of PV by various siRNAs induced a significant decrease in the expression of endogenous NCC, confirming the cellular specificity of the mechanism linking PV and NCC. In neurons and skeletal muscle cells, PV acts as a cytosolic Ca^{2+} buffer that influences the shape and duration of Ca^{2+} transients (30, 31). Such transients are physiologically involved in the transcriptional regulation of several genes, including transporters (32, 33). The distribution of PV in the early DCT, and the fact that DCT cells are sensitive to purinergic signaling (18), led us to show that ATP induced Ca^{2+} transients in mDCT cells. This ATP-induced Ca^{2+} signal is modulated by PV and regulates the endogenous expression of NCC. These results are consistent with earlier studies showing that ATP increase intracellular Ca^{2+} concentration ($[Ca^{2+}]_i$) and inhibit Na^+ absorption in the distal nephron via luminal P2Y2 receptors (34). Further studies are required to elucidate the link between modifications in the amplitude and/or duration of Ca^{2+} signals on downstream effectors such as kinases and transcription factors in the DCT. Genes down-regulated by Ca^{2+} transients have been identified in *Arabidopsis*, but the mechanisms have not been identified (35, 36).

On the basis of the evidence obtained in mouse and mDCT cells, it is tempting to suggest that PV could play a role in human diseases affecting the distal tubule. The phenotype of $Pvalb^{-/-}$ mice resembles that observed in GS, an autosomal recessive tubulopathy caused by inactivating mutations in the *SLC12A3* gene coding for NCC (37). GS is typically a mild salt-losing disorder, associated with secondary aldosteronism, hypocalciuria, and higher bone density (38). More than 100 mutations in *SLC12A3* have been identified, although up to 40% of GS patients are found to carry only a single mutation. The phenotype of GS is highly heterogeneous, raising the possibility of modifier genes (39). Thus, mutations or variants in *PVALB* could be involved in *SLC12A3*-negative patients with GS or resembling tubulopathies or participate in the phenotype variability. Inherited or acquired variation in PV may also play a role in NaCl handling in the DCT and the individual response to thiazides.

Methods

Animal Studies. Experiments were performed on age- and gender-matched *Pvalb* littermates kept on a C57BL/6J×Sv129 background (5, 6). Blood samples were obtained after anesthesia. The endogenous lithium clearance was used as an inverse measure of PT Na^+ reabsorption (20). Parameters were obtained at baseline and after injection of furosemide or HCTZ (10 mg/kg, s.c.). The effect of NaCl supplementation was investigated in $Pvalb^{-/-}$ mice receiving either tap water or 0.9% NaCl/0.1% KCl in drinking water for 48 h or 2 weeks. All protocols complied with the National Research Council Guide for the Care and Use of Laboratory Animals and were approved by the local Ethics Committee.

Analytic Procedures. Plasma and urine parameters were measured with a Synchron CX5 analyzer (Beckman Coulter, Fullerton, CA), an i-STAT analyzer (Abbott Diagnostics, Ottignies, Belgium), an osmometer (Fiske, Needham Heights, MA), or a flame photometer

as appropriate. Plasma $1,25(OH)_2$ vitamin D_3 (BARC, Ghent, Belgium) and urine aldosterone (DPC, Humbeek, Belgium) were measured by RIA.

RT-PCR and Real-Time Quantitative PCR. Samples were homogenized in TRIzol. Total RNA was treated with DNase I and reverse-transcribed by using SuperScript II Rnase H (Invitrogen, Carlsbad, CA). The primers are listed on SI Table 5. RT-PCR detection was performed with platinum *Taq*DNA polymerase (Invitrogen) for 32 cycles, and PCR products were visualized on a 1.5% agarose gel. Real-time quantitative PCR analyses were performed in duplicate by using iQ SYBR Green Supermix (Bio-Rad, Hercules, CA) (40). PCR conditions were 94°C for 3 min followed by 40 cycles of 30 s at 95°C, 30 s at 61°C, and 1 min at 72°C. The relative changes in target gene/GAPDH mRNA ratio were determined by the formula: $2^{\Delta\Delta ct}$ (40).

Antibodies. Antibodies against PV (Santa Cruz Biotechnology, Santa Cruz, CA), NCC (a gift of D. H. Ellison, Oregon Health and Science University, Portland, OR), AQP2 (Alomone, Jerusalem, Israel), uromodulin (Biodesign International, Saco, ME), CB-D28k (Swant, Bellinzona, Switzerland), and GFP (Westburg, Leusden, Netherlands) were used.

Immunoblotting Analyses. Membrane and cytosol extraction and immunoblotting were performed as described (40). The homogenates were centrifuged at $1,000 \times g$ for 15 min at 4°C, and the resulting supernatant was centrifuged at $100,000 \times g$ for 60 min at 4°C. Protein concentrations were determined with the bicinchoninic acid assay using BSA as standard.

Immunostaining. Kidney samples were fixed in 4% formaldehyde. Six-micrometer paraffin sections were successively incubated in 0.3% H_2O_2, 10% normal serum, primary antibodies diluted in PBS containing 2% BSA, biotinylated secondary antibodies, avidin-biotin peroxidase, and aminoethylcarbazole or Texas red-conjugated and FITC-conjugated avidin (Vector Laboratories, Burlingame, CA). Sections were viewed under a DMR microscope coupled to a DC300 digital camera (Leica, Heerbrugg, Switzerland).

Bone Analysis. A high-resolution scanner (pQCT Research XCT-SA+; Norland-Stratec, Pforzheim, Germany) was used to analyze the geometric and densitometry parameters of the tibia in anesthetized *Pvalb* mice (ref. 41 and SI Text).

Human Kidney Samples. Samples from human kidneys prepared for transplantation were used for RNA and protein extraction and immunohistochemistry as described. The use of these human samples was approved by the local Ethical Review Board.

Cell Culture. The immortalized mDCT cells were kindly provided by P. A. Friedman (University of Pittsburgh School of Medicine, Pittsburgh, PA). The cells have been previously characterized as a model for the thiazide-sensitive Na^+ and Ca^{2+} transport occurring in the DCT (16, 17). The cells were grown in DMEM/Ham's F-12 media (Lonza, Verviers, Belgium) supplemented with 5% FCS (Lonza), 2 mM L-glutamine (Invitrogen), and a mixture of penicillin/streptomycin in a humidified atmosphere of 95% air-5% CO_2 at 37°C. Cell passages 20–35 were used. The knockdown of PV was performed with 20 nM of double-stranded Silencer siRNA (Ambion, Lennik, Belgium) introduced into mDCT cells with Lipofectamine 2000 (Invitrogen). RNA was extracted 48 h after transfection. mDCT cells stably transfected with PV were obtained after cloning the mouse PV sequence into a pAcGFP1-C In-Fusion Ready Vector encoding a GFP (Westburg, Leusden, The Netherlands) and tranfection using FuGENE 6 Reagent (Roche, Indianapolis, IN). When appropriate, mDCT cells were treated with EGTA-AM (10 μM) for 6 h and after 4 h with(out) EGTA-AM, cells were stimulated with ATP 10 μM for 6 min every hour for 6 h.

$[Ca^{2+}]_i$ Measurements. Cytosolic free Ca^{2+} ($[Ca^{2+}]_i$) concentration was measured in individual mDCT cells using FURA2-AM as described (ref. 42 and SI Text).

Data Analyses. Data are means ± SEM. Statistical comparisons were tested by two-tailed Student's *t* test (Prism software; GraphPad, San Diego, CA).

1. Ikura M, Ames JB (2006) *Proc Natl Acad Sci USA* 103:1159–1164.
2. Berridge MJ, Bootman MD, Roderick HL (2003) *Nat Rev Mol Cell Biol* 4:517–529.
3. Bhattacharya S, Bunick CG, Chazin WJ (2004) *Biochim Biophys Acta* 1742:69–79.
4. Celio MR (1990) *Neuroscience* 35:375–475.
5. Schwaller B, Dick J, Dhoot G, Carroll S, Vrbova G, Nicotera P, Pette D, Wyss A, Bluethmann H, Hunziker W, *et al.* (1999) *Am J Physiol* 276:C395–C403.
6. Raymackers JM, Gailly P, Schoor MC, Pette D, Schwaller B, Hunziker W, Celio MR, Gillis JM (2000) *J Physiol (London)* 527:355–364.
7. Schwaller B, Tetko IV, Tandon P, Silveira DC, Vreugdenhil M, Henzi T, Potier M-C, Celio MR, Villa AEP (2004) *Mol Cell Neurosci* 25:650–663.
8. Lewis DA, Hashimoto T, Volk DW (2005) *Nat Rev Neurosci* 6:312–324.
9. Bindels RJ, Timmermans JA, Hartog A, Coers W, van Os CH (1991) *J Am Soc Nephrol* 2:1122–1129.
10. Loffing J, Loffing-Cueni D, Valderrabano V, Kläusli L, Hebert SC, Rossier BC, Hoenderop JGJ, Bindels RJM, Kaissling B (2001) *Am J Physiol* 281:F1021–F1027.
11. Moreno E, Cristobal PS, Rivera M, Vazquez N, Bobadilla NA, Gamba G (2006) *J Biol Chem* 281:17266–17275.
12. Hoenderop JGJ, Nilius B, Bindels RJM (2005) *Physiol Rev* 85:373–422.
13. Loffing J, Loffing-Cueni D, Hegyi I, Kaplan MR, Hebert SC, Le Hir M, Kaissling B (1996) *Kidney Int* 50:1180–1190.
14. Adams JS, Song CF, Kantorovich V (1999) *Ann Intern Med* 130:658–660.
15. Nicollet-Barousse L, Blanchard A, Roux C, Pietri L, Bloch-Faure M, Kolta S, Chappard C, Geoffroy V, Morieux C, Jeunemaître X, *et al.* (2005) *J Bone Miner Res* 20:799–808.
16. Gesek FA, Friedman PA (1992) *J Clin Invest* 90:429–438.
17. Gesek FA, Friedman PA (1995) *Am J Physiol* 268:F89–F98.
18. Dai LJ, Kang HS, Kerstan D, Ritchie G, Quamme GA (2001) *Am J Physiol* 281:F833–F840.
19. Câmpean V, Kricke J, Ellison D, Luft FC, Bachmann S (2001) *Am J Physiol* 281:F1028–F1035.
20. Nijenhuis T, Vallon V, van der Kemp AWCM, Loffing J, Hoenderop JGJ, Bindels RJM (2005) *J Clin Invest* 115:1651–1658.
21. Nijenhuis T, Hoenderop JGJ, Loffing J, van der Kemp AWCM, van Os CH, Bindels RJM (2003) *Kidney Int* 64:555–564.
22. Lee C, Shang S, Lai L, Yong K, Lien YH (2004) *Am J Physiol* 287:F1164–F1170.
23. Loffing J, Vallon V, Loffing-Cueni D, Aregger F, Richter K, Pietri L, Bloch-Fauré M, Hoenderop JGJ, Schull GE, Meneton P, *et al.* (2004) *J Am Soc Nephrol* 15:2276–2288.
24. Schultheis PJ, Lorenz JN, Meneton P, Nieman ML, Riddle TM, Flagella M, Duffy JJ, Doetschman T, Miller ML, Shull GE (1998) *J Biol Chem* 273:29150–29155.
25. Farre-Castany MA, Schwaller B, Gregory P, Barski J, Mariethoz C, Eriksson JL, Tetko IV, Wolfer D, Celio MR, Schmutz I, *et al.* (2007) *Behav Brain Res* 178:250–261.
26. Morris RG, Hoorn EJ, Knepper MA (2006) *Am J Physiol* 290:F1416–F1420.
27. Wilson FH, Disse-Nicodeme S, Choate KA, Ishikawa K, Nelson-Williams C, Desitter I, Gunel M, Milford DV, Lipkin GW, Achard JM, *et al.* (2001) *Science* 293:1107–1112.
28. Yang CL, Zhu X, Wang Z, Subramanya AR, Ellison DH (2005) *J Clin Invest* 115:1379–1387.
29. Peng JB, Bell PD (2006) *Kidney Int* 69:2116–2118.
30. Schwaller B, Meyer M, Schiffmann S (2002) *Cerebellum* 1:241–258.
31. Gailly P (2002) *Biochim Biophys Acta* 1600:38–44.
32. Dolmetsch RE, Xu K, Lewis RS (1998) *Nature* 392:933–936.
33. Pigozzi D, Ducret T, Tajeddine N, Gala JL, Tombal B, Gailly P (2006) *Cell Calcium* 39:401–415.
34. Leipziger J (2003) *Am J Physiol* 284:F419–F432.
35. Kaplan B, Davydov O, Knight H, Galon Y, Knight MR, Fluhr R, Fromm H (2006) *Plant Cell* 18:2733–2748.
36. Ikura M, Osawa M, Ames JB (2002) *BioEssays* 24:625–636.
37. Simon DB, Nelson-Williams C, Bia MJ, Ellison D, Karet FE, Molina AM, Vaara I, Iwata F, Cushner HM, Koolen M, *et al.* (1996) *Nat Genet* 12:24–30.
38. Peters M, Jeck N, Reinalter S, Leonhardt A, Tonshoff B, Klaus GG, Konrad M, Seyberth HW (2002) *Am J Med* 112:183–190.
39. Riveira-Munoz E, Chang Q, Bindels RJ, Devuyst O (2007) *Pediatr Nephrol* 22:326–332.
40. Jouret F, Bernard A, Hermans C, Dom G, Terryn S, Leal T, Lebecque P, Cassiman JJ, Scholte BJ, De Jonge HR, *et al.* (2007) *J Am Soc Nephrol* 18:707–718.
41. Nzeussu A, Dienst D, Haufroid V, Depresseux G, Devogelaer JP, Manicourt DH (2006) *Bone* 38:394–399.
42. Gailly P (1998) *Cell Calcium* 24:293–304.

6